Use of chemometrics and laser-induced breakdown spectroscopy for quantitative analysis of major and minor elements in aluminium alloys

Doucet, François R.; Belliveau, Thomas F.; Fortier, Jean-Luc; Hubert, Joseph

Publisher's version / Version de l'éditeur:
https://doi.org/10.1366/000370207780220813
Applied Spectroscopy, 61, 3, pp. 327-332, 2007-03-01

Use of Chemometrics and Laser-Induced Breakdown Spectroscopy for Quantitative Analysis of Major and Minor Elements in Aluminum Alloys

FRANÇOIS R. DOUCET, THOMAS F. BELLIVEAU, JEAN-LUC FORTIER, and JOSEPH HUBERT*

Université de Montréal, Faculté des arts et des sciences, Département de chimie, P.O. BOX: 6128 station A, Montréal, Québec, CANADA H3C 3J7 (F.R.D., J.H.); and Alcan Inc., Arvida Research and Development Center (ARDC), 1955, Mellon Blvd., Building 110, Jonquière, Québec, CANADA G7S 4K8 (T.F.B., J.-L.F.)

In the present work, quantitative analysis of major and minor elements in aluminum alloys is investigated using chemometrics and laser-induced plasma spectroscopy with a commercially available laser-induced breakdown (LIBS) spectrometer. Multivariate calibrations use the entire signal matrix for all elements in a single multivariate regression model. This enables accounting for the correlation between variables often referred to as matrix effects in conventional univariate modeling. Modeling the entire signal matrix improves robustness over traditional univariate calibration since it can compensate for matrix effects. Several nonlinear data pretreatment methods have been used to correct for nonlinear behaviors of the analytical signals prior to performing the multivariate calibration. The use of multivariate calibration in combination with cubic implicit nonlinear data pretreatment showed the most accurate results. The accuracy reported with the developed multivariate calibration is better than 5% for the major alloying elements. Based on the results obtained, the use of chemometrics and laser-induced plasma spectroscopy have been successfully applied to the quantitative analysis of major and minor alloying elements in aluminum.

Index Headings: **Laser-induced breakdown spectroscopy; Chemometrics; Aluminum alloys; Multivariable.**

INTRODUCTION

Laser-induced breakdown spectroscopy (LIBS) is a well-known technique for the direct analysis of a wide variety of materials. For the elemental analysis of metals, the increased excitation energy available in the laser pulse compared to an electrical spark should, in principle, eliminate analytical problems commonly referred to as matrix effects. Previous work suggests that these matrix effects are reduced, but not eliminated.[1] Many papers have been published on the quantitative analysis of aluminum alloys[1–16] using univariate prediction models constructed with classical least-squares regression between a dependent variable (signal for an element) and an independent variable (concentration of the element). The drawback with univariate prediction models is that they are sensitive to matrix effects. In the quantitative multi-elemental analysis of metallic alloys of aluminum, iron, or copper, the use of a matrix-matching univariate calibration method is often used to compensate for matrix effects.[1] A matrix-matching analysis method implies the use of standards having a matrix similar to the sample being analyzed. In an industrial environment, the use of the matrix-matching method can become tedious for given analytical requirements. For example, the accuracy of the emission spectroscopy analysis may be compromised if matrix-matched standards are not available and wet chemical analyses may be required for verification purposes. In addition, the preparation and certification of new matrix-matched standards may involve major efforts and introduce significant delays. The present paper examines the use of chemometrics as a multivariate regression tool to compensate for matrix effects and add robustness to the matrix-matched method for the quantitative analysis of major and minor elements in alloys.

The initial work on multivariate calibration for quantitative analysis by laser-induced breakdown spectroscopy was realized by Palanco et al.,[17] following earlier work by Slickers[18] on spark-optical emission spectroscopy (spark-OES). Other researchers have also successfully applied multivariate calibration in LIBS for quantitative analysis of samples in various matrices.[19–23] In general, it is possible to obtain a significant[19–23] or a large[17] gain in accuracy.

Generally, one can express the net intensity of an emission line $\mathbf{I}_A$, of an analyte A, at the wavelength $\boldsymbol{\lambda}_A$, by Eq. 1. The net intensity $\mathbf{I}_A$, is a function of the analyte concentration $\mathbf{C}_A$, the analysis time **t**, factors related to source **S**, and matrix **M** conditions. In the ideal case, the contribution of the matrix **M** to the analytical signal should be negligible; unfortunately, in reality, this is not often the case:

$$\mathbf{I}_A(\lambda_A) = f(\mathbf{C}_A, \mathbf{t}, \mathbf{S}, \mathbf{M}) \quad (1)$$

The contributions to the analytical signal known as matrix effects (**M**) arise from physical, chemical, and/or spectral interferences. For quantitative multi-elemental analysis of over 26 elements in aluminum alloys, it becomes nearly impossible to consider the contribution of all matrix effects to the analytical signal and compensate for them. The goal of using a multivariate calibration is to consider simultaneously the entire analytical signal available to construct a more robust calibration model instead of trying to correct the individual contributions of matrix effects to the analytical signal in a univariate calibration model.

EXPERIMENTAL

All LIBS measurements were performed with a Thermo ARL (Ecublens, Vaud, Switzerland) Laser-Spark 7011 spectrometer (a standard ThermoARL 4460 OES spectrometer with additional electronics for time-resolved spectroscopy). The Paschen–Runge 1-meter vacuum spectrometer has a 1080 grooves mm^{-1} grating optimized for 600 nm and the emission lines for the different elements studied are listed in Table I (these emission lines are the standard analytical lines used in

Received 26 July 2006; accepted 4 January 2007.
* Author to whom correspondence should be sent. E-mail: Joseph.Hubert@UMontreal.CA.

0003-7028/07/6103-0327$2.00/0

TABLE I. Configuration of the Paschen–Runge spectrometer.

Element name	Wavelength (nm)	Diffraction order	Delay (μs)	Gate (ms)
Cu–H[a]	510.55	1	27	0.050
Cu–L[b]	324.75	2	8	50[c]
Fe	371.99	2	27	0.050
Mg–H	382.93	1	8	50
Mg–L	285.21	2	8	50
Mn–H	346.03	1	8	50
Mn–L	403.45	2	27	0.050
Ni	341.48	2	8	50
Si–H	390.55	2	8	50
Si–L	288.16	2	27	0.050
Ti	337.28	2	8	50

[a] –H refers to the line used for major concentration determination.
[b] –L refers to the line used for trace and minor concentration determination.
[c] Typical gate time with the use of switch board on PMTs. The delay refers to time difference between the laser pulse and the beginning of the integration.

the traditional spark-OES). The Laser-Spark 7011 uses a photomultiplier tube (PMT) for each line with matched sensitivity for the wavelength. The PMT's time-resolved signal is assured by a switch board in order to block the first 8 μs of the LIBS signal related to the strong continuum emission of the plasma in this time domain. Further time-resolved signals are selected by digitizing the analog signal using a sample and hold electronic card with a V-F converter. The Laser-Spark 7011 has a Quantel Brillant ARL Nd-YAG laser as the excitation source that can supply a fundamental wavelength (1064 nm, 5 ns full-width at half-maximum (FWHM)) with 250 mJ pulses at a frequency of 20 Hz. All samples were prepared on a Herzog (Osnabruck, Germany) HN-2F milling machine as normally done prior to spark-OES analysis.

The optimization of excitation conditions and instrument parameters for the analysis are presented elsewhere.[25,26] The 250 mJ laser beam is focused 13 mm behind the sample surface and the diameter of the spot produced is 0.8 mm. These conditions correspond to a laser fluence of around 40 J cm^{-2}. During analysis, an argon (ICP grade >99.999%) flow of 5 L min^{-1} is maintained in the ablation chamber of the Laser-Spark 7011. Also during analysis, the Laser-Spark rotates the sample table to produce a 5 mm diameter analysis region. The analysis conditions on the Laser-Spark 7011 are 8 s argon purge, 10 s surface preparation (200 laser shots), and 15 s integration (300 laser shots).

In order to construct the calibration model, over 260 aluminum standards (certified reference materials) were used. These standards were of two types (1) "binary standards", and (2) "alloy standards" or matrix-matched calibration standards. The "binary standards" are made from one element in an aluminum matrix; on the other hand the "alloy standards" are made with all elements within the composition limits of a given aluminum alloy type. Alcan Inc, Arvida Research and Development Centre (Jonquière, Quebec, Canada), supplied all aluminum standards and samples.

All chemometrics calculations were performed with Matlab 6.5 (The MathWorks, Inc., Natick, MA) using custom algorithms developed for the experiments.

RESULTS AND DISCUSSIONS

Table II shows the concentration range of the different elements considered in the construction of the multivariate calibration model. The certified values of the 260 calibration

TABLE II. Concentration range of alloying elements in the aluminum calibration samples.

Element	Concentration range (%w/w)
Fe	0.001–0.76
Cu	0.0001–9.86
Mg	0.0001–9.95
Mn	0.0007–5.12
Ni	0.0004–5.13
Si	0.038–12.96
Ti	0.001–0.56

samples can be obtained upon request. The concentration ranges shown in Table II cover most of the major aluminum alloying elements, i.e., Si, Mg, Mn, Cu, Fe, and Ti (Zn is excluded). The wide concentration range on such a large number of elements results in significant matrix modifications of the chemical, physical, and metallurgical properties of the aluminum standards.

Figure 1 shows the extent of matrix effects on iron determination by comparing the response of alloy standards to the iron binary standards response. The iron binary standards can be considered free of any matrix effect. This is confirmed by noting that all binary data points (intensity versus concentration) fall directly on the third degree binary regression line with a multiple regression coefficient, R^2, of 0.998. However, the alloy standards signals do not follow the same curve and show significantly more scatter (Fig. 1) than the binary data point line. For the same certified iron concentration, an alloy standard will produce a lower signal than a binary standard. When using a univariate calibration model, these matrix effects can be partially corrected with a matrix-matching technique, for example, using a two-point standardization with matrix-matched alloy standards.[1,24] The present work will use a chemometrics multivariate calibration in order to correct for these matrix effects by modeling the entire signal matrix with the certified concentrations of all of the alloying elements.

For spark-OES, there are no theoretical calibration curves that can be used for practical purposes, and although the response may be linear at lower concentrations, standard practice in the industry expresses calibration curves as third-order polynomials (over the whole calibration range, or in sections). The use of a Paschen–Runge spectrometer implies that the signal measured by the spectrometer is related to the integrated area of an emission line. Neither the net area nor the net height of an emission line can be measured since the underlying continuum cannot be measured. The generally lower intensity for alloy samples compared to binary samples is also observed in traditional spark-OES. Whether this "matrix effect" is due to suppression of analytical signal or background signal cannot be determined with the current configuration. The source of this "matrix effect" is beyond the scope of this communication. These interactions between variables can be correlated with the use of multivariate calibration.

The two matrices of independent and dependent variables used to construct the multivariate model are presented in Fig. 2 after an auto-scaling preprocessing that extracts pattern variation in the two matrices for a better visual comparison. The binary standards are easily identified in the two matrices as the "peaks" appearing from the middle to the rear of the matrices. The alloy standards appear at the front of the matrices

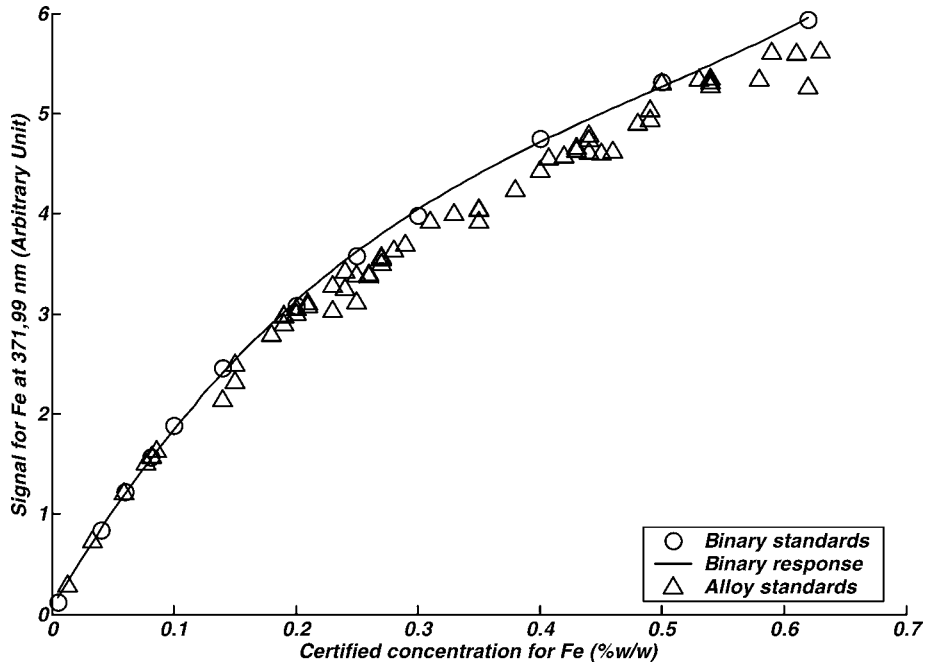

FIG. 1. Comparison between the binary calibration samples response and the alloy standards response.

and show multiple, significantly smaller "peaks". The similarities between the two variable matrices are easily recognized, but it is difficult to predict how the data of these two matrices can be correlated to produce an accurate prediction model. As often observed in LIBS and other atomic emission spectroscopy (AES) techniques, the analytical signal variation with concentration can be strongly nonlinear, both for major and minor constituents, as is seen in Fig. 1. This nonlinearity must be treated prior to the construction of the multivariate calibration model.[27] Failure to treat the nonlinear behavior before constructing the multivariate calibration model leads to predicted concentrations showing a systematic nonlinear deviation pattern when compared to the certified concentration of the aluminum samples in the training set (Fig. 3). Examination of the corresponding residuals plot suggests that the multilinear regression model failed because of the nonlinearity of the analytical signals against concentration (Fig. 3).

Different approaches to manipulating the raw data with mathematical pretreatments can be used to handle nonlinearity.[28–39] Neural network genetic algorithms can also be applied to try to correct for the nonlinearity.[40,41] The problem with these approaches is that the complexity of the algorithms can increase significantly. The approach that gives the best performance on the current data set is the implicit nonlinear correction developed by Berglund,[42] while keeping the algorithm as simple as possible. This method consists of adding to the original spectral data the squares and the cubes of these data, in order to compensate for the quadratic and cubic signal dependence on concentration.

The equation for multi-linear regression construction is as follows:

$$\mathbf{C} = \mathbf{XB} \tag{2}$$

where $\mathbf{C}$ is the concentration matrix ($n \times m$, where the n rows correspond to the calibration standards and m columns for each element concentration) for the calibration standards. $\mathbf{X}$ is the signal matrix for the corresponding calibration standards ($n \times k$), where the n rows correspond to the calibration standards and k columns correspond to each line mounted on the spectrometer. $\mathbf{B}$ is the $k \times m$ matrix corresponding to the multilinear regression coefficients that correlated the analytical signals from each line mounted on the spectrometer (row wise) with the concentration of all elements (column wise).

The matrix $\mathbf{B}$ can be calculated with the following equation:

$$\mathbf{B} = (\mathbf{X}'\mathbf{X})^{-1}\mathbf{X}'\mathbf{C} \tag{3}$$

When the matrix $\mathbf{B}$ is known, the concentration of unknown samples can be evaluated with

$$\mathbf{C}_{\text{unknown}} = \mathbf{X}_{\text{unknown}}\mathbf{B}' \tag{4}$$

Figure 4 shows the predicted concentration using the multilinear regression model with cubic implicit compensation for the major alloying elements; this approach gives good results when compared to Fig. 3, where no implicit nonlinear correction is used. Using the cubic implicit nonlinear correction generates predicted concentrations for the training set in good agreement with the certified concentration for all major alloying elements in the aluminum alloys examined. This is also confirmed by examination of the corresponding residuals plot of Fig. 4, which presents a scattered pattern instead of the systematic pattern observed in the residuals plot of Fig. 3.

Table III summarizes the results of the evaluation of different multivariate calibration models: multi-linear regression (MLR), principal component regression (PCR), and partial least square regression (PLSR) with or without using implicit nonlinear correction as a data pretreatment. To compare the different models and the use of different data pretreatments, the predictive residual error sum-of-squares (PRESS), the root mean square error of calibration (RMSEC), the root mean square error of prediction (RMSEP), and the multiple correlation coefficient (R^2) have been evaluated. These

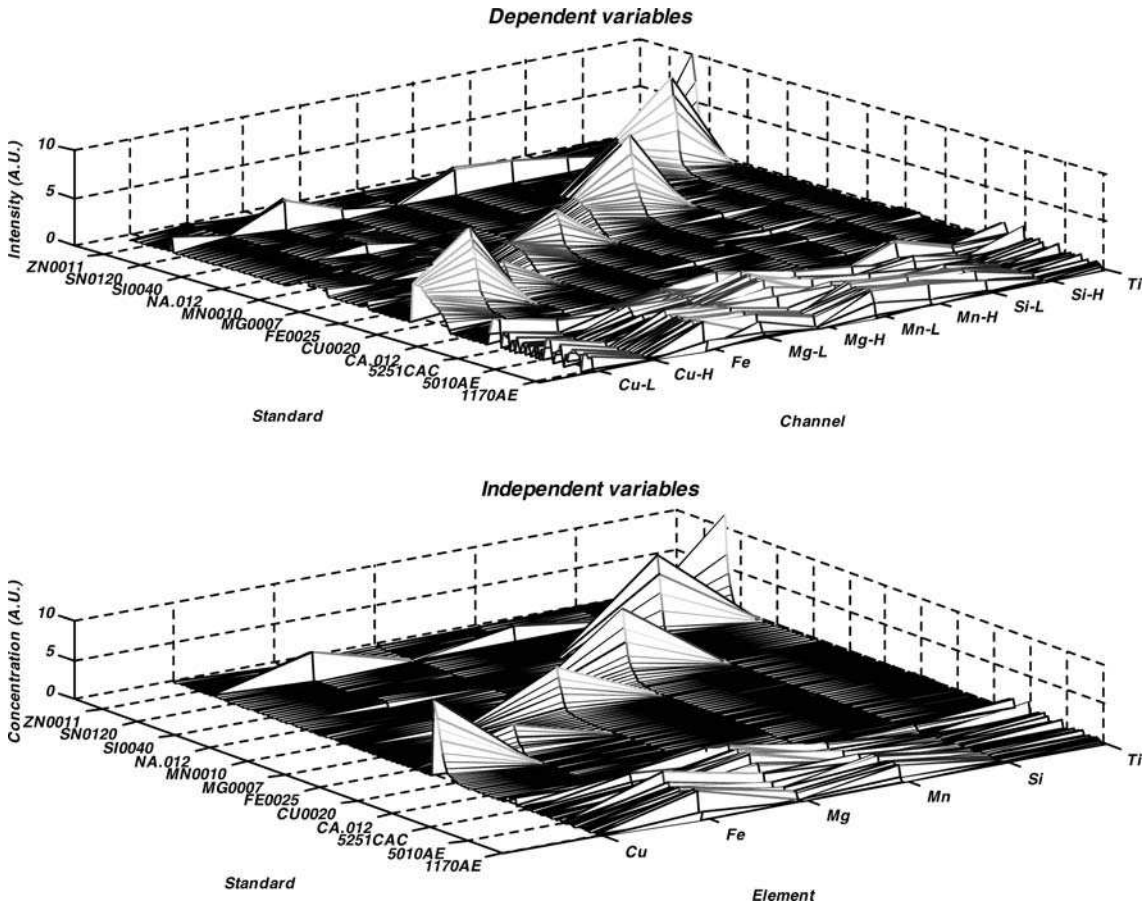

FIG. 2. Graphical representation of the dependent variables (260 × 10) and the independent variables (260 × 6) after an auto scaling preprocessing.

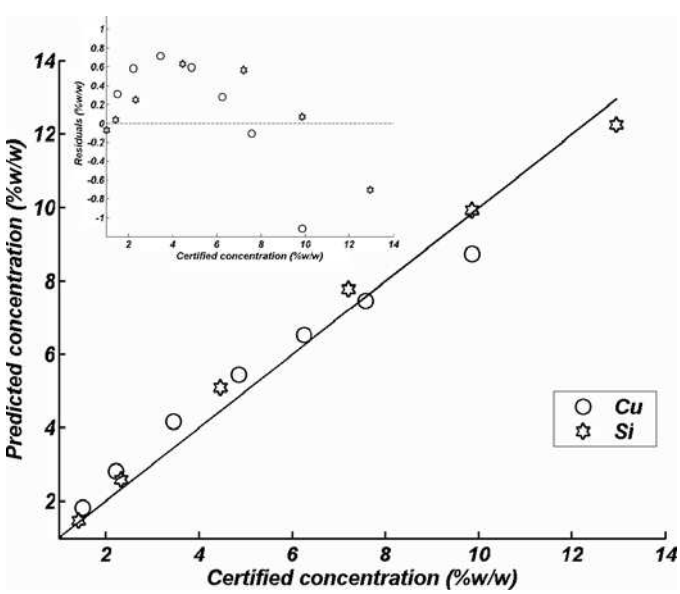

FIG. 3. Comparison between the predicted concentration by a multi-linear regression model and the certified concentration of Cu and Si as major constituents (solid line: 1:1 correspondence) and corresponding residuals plot.

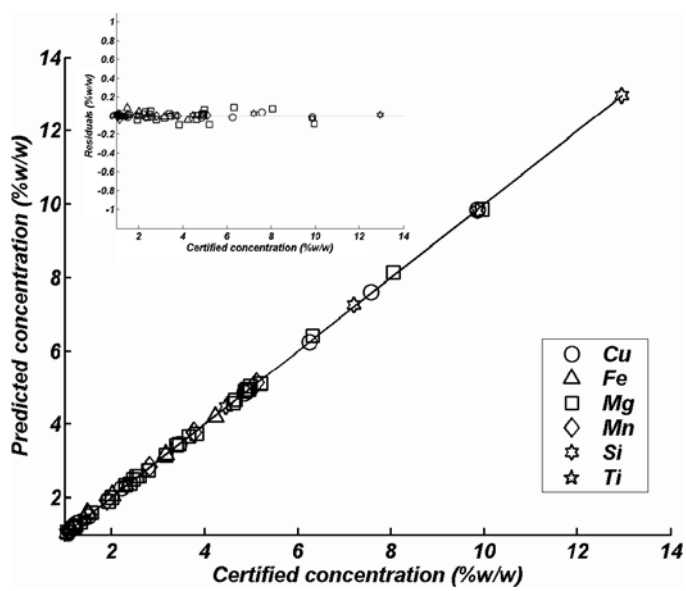

FIG. 4. Comparison between the predicted concentration by a multi-linear regression model and the certified concentration of Cu, Fe, Mg, Mn, Si, and Ti as major constituents using a cubic implicit nonlinear correction (solid line: 1:1 correspondence) and corresponding residuals plot.

TABLE III. Multivariate statistics for the different multivariable calibration models using different nonlinear correction preprocessing.[a]

Multivariate model type	Nonlinear correction	PRESS	RMSEC	RMSEP	R^2
MLR	None	0.0304	1.12	1.68	0.979
MLR	Quadratic	0.0639	0.379	0.748	0.998
MLR	Cubic	0.000885	0.231	0.214	0.999
PCR nLV = 6	None	9.99	6.85	11.0	0.372
PCR nLV = 15	Quadratic	1.58	2.84	4.20	0.873
PCR nLV = 17	Cubic	0.549	2.31	3.31	0.911
PLSR nLV = 20	None	0.0299	1.33	1.75	0.958
PLSR nLV = 21	Quadratic	0.0204	0.823	0.946	0.976
PLSR nLV = 23	Cubic	0.0711	1.43	2.03	0.955

[a] PRESS = predictive residual error sum-of-squares, RMSEC = root mean square error of calibration, RMSEP = root mean square error of prediction, R^2 = multiple regression coefficient, MLR = multi-linear regression, PCR = principal component regression, PLSR = partial least square regression, nLV = number of latent variables.

parameters were also evaluated for different data scaling techniques, such as range scaling, mean scaling, and auto scaling (data not shown).

As expected, the use of preliminary data scaling does not improve the predictive ability (i.e., RMSEP) of any of the multivariate regression models evaluated in the present work. Even the use of a floating intercept was examined, but showed no predictive ability improvement (RMSEP) in the multivariate regression models (data not shown). This situation is probably caused by the orthogonality (i.e., scalar for each element) of the dependent variables (i.e., signals) obtained from the Paschen–Runge spectrometer in comparison to collinear data (i.e., peak defined by a certain number of pixels for each element), like the signals obtained with an Échelle spectrometer.

In Table III we see that the use of quadratic and cubic implicit nonlinear corrections gives significant improvement in the predictive ability of the multivariate regression model. These improvements are reflected in the reduction of the PRESS, RMSEC, and RMSEP values and an R^2 approaching unity. The best performance is obtained by MLR with the use of a cubic implicit nonlinear correction pretreatment.

Refining of the MLR model with cubic implicit nonlinear correction using a cross-validation genetic algorithm for selection of the most relevant aluminum standards and evaluating the robustness of the model each time allows estimation of the accuracy obtained with the multivariate prediction model. Accuracies obtained for the major (i.e., more than 1% w/w) and some minor alloying elements using the MLR model with a cubic implicit nonlinear data pretreatment are presented in Table IV. For presentation reasons, we limit the number of validation standards to only critical alloys that exhibit strong "matrix effects" in a traditional univariate calibration model. It is noticed that the accuracy obtained for the major alloying elements is generally better than 5%. The worst performances in terms of accuracy are observed in alloy 5182 (i.e., Al–Mg alloy) for Cu, Fe, Si, and Ti; however, in this case, the alloying elements are only present at minor concentrations (i.e., between 0.1 and 1% w/w). Those accuracy performances are significantly better than those obtained without the use of cubic implicit nonlinear data pretreatment, as reported in the second half of Table IV.

Significant lack of accuracy problems were observed for trace and some minor elements (data not shown). This deficiency can be explained by the lack of information on trace element concentrations in some standards, particularly the binary standards, where the concentrations of all the elements other then the binary elements are not certified. The incomplete certification data does not permit the model to determine whether the variation in intensities arises from interferences or actual presence of the trace element, so accuracy is compromised. Knowledge of the fabrication history of the standards and the presence of multiple spectral lines for some major elements allows estimation of some of the unknown values, but not all. Complete chemistry calibration data would be necessary to resolve this issue. Further work is needed to complete the evaluation of chemometrics models for the quantitative analysis of most minor and trace alloying elements in aluminum.

CONCLUSION

Chemometrics coupled with LIBS is a suitable combination for the quantitative analysis of alloying elements in aluminum alloys. The use of implicit nonlinear correction as a data pretreatment technique aids in the construction of the multivariate calibration model. The accuracy obtained for the aluminum standards test set demonstrates the ability of a multivariate calibration model to compensate for matrix effects and thus increase the robustness of LIBS quantitative analysis

TABLE IV. Relative accuracy obtained from a multi-linear regression model for different alloys in the test set.

Alloys	Accuracy Cu (%)	Accuracy Fe (%)	Accuracy Mg (%)	Accuracy Mn (%)	Accuracy Si (%)	Accuracy Ti (%)
3104	1.8	1.7	0.74	0.75	5.0	3.2
5182	5.7[a]	7.7[a]	0.65	1.7	6.9	5.7
6111	1.1	5.8[a]	0.094	4.3	3.9	0.39
3104[b]	3.4	8.5	6.3	0.69	2.5	1.9
5182[b]	9.1	2.6	4.6	3.0	21	6.0
6111[b]	17	12.0	0.1	5.3	5.8	1.8

[a] Minor elements in the alloy.
[b] Accuracy value for the multi-linear model without the use of cubic implicit nonlinear data pretreatment.

of aluminum alloys. However, the certification of minor and trace elements in some of the key aluminum standards is essential for a further investigation of quantitative analysis of minor and trace elements in aluminum alloys by LIBS. Moreover, evaluation of other emission lines giving a more linear intensity concentration response than those used in the present work should be considered for improvement of the analytical results.

ACKNOWLEDGMENTS

This work was supported by an infrastructure grant from the Canadian Foundation for Innovation and by the National Sciences and Engineering Research Council of Canada (NSERC). FRD is grateful to Alcan Inc., NSERC, and Université de Montréal for scholarships.

1. F. R. Doucet, T. F. Belliveau, J.-L. Fortier, and J. Hubert, J. Anal. At. Spectrom. **19,** 499 (2004).
2. L. St-Onge, M. Sabsabi, and P. Cielo, Spectrochim. Acta, Part B **53,** 407 (1998).
3. L. Paksy, B. Nemet, A. Lengyel, L. Kozma, and J. Czekkel, Spectrochim. Acta, Part B **51,** 279 (1996).
4. M. Sabsabi and P. Cielo, J. Anal. At. Spectrom. **10,** 643 (1995).
5. P. N. Wang, Q. Pan, N. H. Cheung, and S. C. Chen, Appl. Spectrosc. **53,** 205 (1999).
6. N. Andre, C. Geertsen, J. L. Lacour, P. Mauchien, and S. Sjostrom, Spectrochim. Acta, Part B **49,** 1363 (1994).
7. C. Geertsen, J. L. Lacour, P. Mauchien, and L. Pierrard, Spectrochim. Acta, Part B **51,** 1403 (1996).
8. B. C. Castle, K. Talabardon, B. W. Smith, and J. D. Winefordner, Appl. Spectrosc. **52,** 649 (1998).
9. A. Ciucci, M. Corsi, V. Palleschi, S. Rastelli, A. Salvetti, and E. Tognoni, Appl. Spectrosc. **53,** 960 (1999).
10. V. Detalle, R. Héon, M. Sabsabi, and L. St-Onge, Spectrochim. Acta, Part B **56,** 1011 (2001).
11. M. Basko, T. Lower, V. N. Kondrashov, A. Kendl, R. Sigel, and J. Meyertervehn, Phys. Rev. E **56,** 1019 (1997).
12. C. Y. Cote, J. C. Kieffer, and O. Peyrusse, Phys. Rev. E **56,** 992 (1997).
13. A. Saemann, K. Eidmann, I. E. Golovkin, R. C. Mancini, E. Andersson, E. Forster, and K. Witte, Phys. Rev. Lett. **82,** 4843 (1999).
14. A. K. Rai, H. Zhang, F. Y. Yueh, J. P. Singh, and A. Weisburg, Spectrochim. Acta, Part B **56,** 2371 (2001).
15. B. Le Drogoff, J. Margot, M. Chaker, M. Sabsabi, O. Barthélemy, T. W. Johnston, S. Laville, F. Vidal, and Y. Von Kaenel, Spectrochim. Acta, Part B **56,** 987 (2001).
16. F. Vidal, S. Laville, T. W. Johnston, O. Barthélemy, M. Chaker, B. Le Drogoff, J. Margot, and M. Sabsabi, Spectrochim. Acta, Part B **56,** 973 (2001).
17. S. Palanco and J. J. Laserna, J. Anal. At. Spectrom. **15,** 1321 (2000).
18. K. Slickers, *Automatic Atomic Emission Spectroscopy* (Brühlsche Universitätsdruckei, Giessen, 1993), 2nd ed.
19. L. Barette and S. Turmel, Spectrochim. Acta, Part B **56,** 715 (2001).
20. L. E. Garcìa-Ayuso, J. Amador-Hermández, J. M. Fernández-Romeroa, and M. D. Luque de Castro, Anal. Chim. Acta **457,** 247 (2002).
21. H. Fink, U. Panne, and R. Neissner, Anal. Chem. **74,** 4334 (2002).
22. A. Jurado-López and M. D. Luque de Castro, Appl. Spectrosc. **57,** 349 (2003).
23. M. Kraushaar, R. Noll, and H.-U. Schmitz, Appl. Spectrosc. **57,** 1282 (2003).
24. P. E. Lemieux and R. H. Black, Can. Spectrosc. **11,** 9 (1966).
25. F. R. Doucet, J.-L. Fortier, T. F. Belliveau, and J. Hubert, Poster at 7th Conference on Laser Ablation, COLA (Hersonissos, Crete, Greece, October 5–10, 2003).
26. F. R. Doucet, Ph.D. Thesis, Faculté des Études Supérieures, Université de Montréal, Montréal, QC, Canada (2004).
27. H. Martens and M. Martens, *Multivariate Analysis of Quality: An Introduction* (John Wiley and Sons, New York, 2001), 1st ed., pp. 153–154.
28. S. Wold, N. Kettaneh-Wold, and B. Skagerberg, Chemom. Intell. Lab. Syst. **7,** 53 (1989).
29. S. Wold, Chemom. Intell. Lab. Syst. **14,** 71 (1992).
30. L. Frank, Chemom. Intell. Lab. Syst. **8,** 109 (1990).
31. B. R. Kowalski, S. Sekulic, Z. Wang, S. E. Lee, and B. R. Holt, Anal. Chem. **65,** 835 (1993).
32. A. Höskuldsson, J. Chemom. **6,** 307 (1992).
33. V.-M. Taavitsainen and P. Korhonen, Chemom. Intell. Lab. Syst. **14,** 185 (1992).
34. V.-M. Taavitsainen and H. Haario, Chemom. Intell. Lab. Syst. **23,** 51 (1994).
35. T. Naes and T. Isaksson, Appl. Spectrosc. **46,** 34 (1992).
36. T. Naes, S. D. Oman, and A. Zube, J. Chemom. **7,** 195 (1993).
37. T. J. McAvoy and S. J. Qin, Comput. Chem. Eng. **16,** 379 (1992).
38. T. R. Holcomb and M. Morari, Comput. Chem. Eng. **16,** 393 (1992).
39. L. Frank, Chemom. Intell. Lab. Syst. **27,** 1 (1995).
40. B. R. Kowalski, Z. Wang, and J.-N. Blank, Anal. Chem. **67,** 1497 (1995).
41. S. D. Brown and T. B. Blank, Anal. Chem. **65,** 3081 (1993).
42. A. Berglund and S. Wold, J. Chemom. **11,** 141 (1997).